Alma Mater Studiorum Università di Bologna
Archivio istituzionale della ricerca

Natural polyamines and synthetic analogs modify the growth and the morphology of Pyrus communis pollen tubes affecting ROS levels and causing cell death

(Article begins on next page)

19 April 2024

Natural polyamines and synthetic analogs modify the growth and the morphology of *Pyrus communis* pollen tubes affecting ROS levels and causing cell death

Iris Aloisi [a], Giampiero Cai [b], Vincenzo Tumiatti [c], Anna Minarini [d], Stefano Del Duca [a],*

[a] *Dipartimento di Scienze Biologiche, Geologiche e Ambientali, Alma Mater Studiorum–Università di Bologna, Via Irnerio 42, Bologna, Italy*
[b] *Dipartimento di Scienze della Vita, Università di Siena, Via Mattioli 4, Siena, Italy*
[c] *Dipartimento di Scienze per la Qualità della Vita, Alma Mater Studiorum–Università di Bologna, Corso d'Augusto 25, Rimini, Italy*
[d] *Dipartimento di Farmacia e Biotecnologie, Alma Mater Studiorum–Università di Bologna, Via Belmeloro 6, Bologna, Italy*

ARTICLE INFO

ABSTRACT

Polyamines (PAs) are small molecules necessary for pollen maturation and tube growth. Their role is often controversial, since they may act as pro-survival factors as well as factors promoting Programmed Cell Death (PCD). The aim of the present work was to evaluate the effect of exogenous PAs on the apical growth of pear (*Pyrus communis*) pollen tube and to understand if PAs and reactive oxygen species (ROS) are interconnected in the process of tip-growth. In the present study besides natural PAs, also aryl-substituted spermine and methoctramine (Met 6-8-6) analogs were tested. Among the natural PAs, Spm showed strongest effects on tube growth. Spm entered through the pollen tube tip, then diffused in the sub-apical region that underwent drastic morphological changes, showing enlarged tip. Analogs were mostly less efficient than natural PAs but BD23, an asymmetric synthetic PAs bearing a pyridine ring, showed similar effects. These effects were related to the ability of PAs to cause the decrease of ROS level in the apical zone, leading to cell death, counteracted by the caspase-3 inhibitor Ac-DEVD-CHO (DEVD). In conclusions, ROS are essential for pollen germination and a strict correlation between ROS regulation and PA concentration is reported. Moreover, an imbalance between ROS and PAs can be detrimental thereby driving pollen toward cell death.

Natural polyamines (PAs) are small widespread polycations known to be necessary for cell growth of all organisms, both prokaryotic and eukaryotic [1]. Putrescine (Put), spermidine (Spd) and spermine (Spm) are the most common PAs, but recently, evidences also showed plants possessing the isomer thermospermine (tSpm) [2]. Most of the biological functions of PAs are associated with their polycationic backbone able to establish electrostatic interactions with anion groups of biological molecules, among which proteins and nucleic acids; also the covalent binding to proteins, catalyzed by transglutaminase (TGase) occurs [1,3,4]. PAs act as regulatory factors in fundamental cellular processes, including cell division, differentiation, gene expression, DNA and protein synthesis, and programmed cell death (PCD), the latter recently reviewed [5,6]. The role of PAs in plant cell death appears to be multifaceted, acting in some instances as pro-survival molecules, whereas in other cases they seem involved in accelerating PCD [5,6].

It is thus not astonishing that the perturbation of PAs homeostasis influences the cellular growth and morphology [7]. In plant cells, PAs are mostly stocked in the vacuole and in the cell wall, but Spm is present also in the nucleus [8], where it is supposed, in addition to a molecular stabilizing role, to act as "radical-scavenger" protecting DNA from reactive oxygen species (ROS) [9,10].

A multifaceted interaction of PAs with ROS and antioxidants is perhaps among the most complex and apparently contradictory physiological and biochemical process in plants [11,12]. Pollen is an useful model to study effect of different factors, as it can be considered like a single cell in culture, it is very sensible, its growth is fast and easy to measure; moreover it is a relevant subject for fertilization and self-incompatibility studies [13]. As a tip-growing cell in which both the cytoskeleton and the tip-localized Ca^{2+} gradient are critical factors driving pollen tube elongation, PAs as well as other factors involved in the regulation of pollen tube dynamics, are likely to take part in the process of pollen tube growth [14,15]. The presence and the active biosynthesis of PAs during germination of Rosaceae pollen, as well as their release from the pollen tube in the external medium, has previously been established [16,17]. In pollen, the homeostasis of PAs is finely regulated and the per-turbation of this balance has provided, over the years, interesting

---

evidences about how PAs carry out some of their functions in the cell. For example, the inhibition of PA biosynthesis was seen to cause a severe inhibition of pollen tube growth and was correlated with reduced binding to cell wall polysaccharides, indicating the essential role of PAs in pollen tube emergence and elongation [18]. Moreover, also an excess of PAs was shown to affect pollen tube causing its arrest, probably because intracellular PAs, that were reported to be also conjugated to cytoskeletal proteins, can regulate cytoskeletal functional properties [14,19].

ROS also play a key role during pollen tube emergence and elongation as they act as wall loosening or stiffening agents [20,21]. In this context, the role of PAs is still largely unknown and in some cases ambiguous, as demonstrated by the double action of PAs in regulation of ROS. In fact, PAs are deaminated by polyamine oxidases (PAOs) in enzymatic reactions that produce hydrogen peroxide (H_2O_2) in the apoplast [22]; on the other hand, different studies have shown the efficient action of PAs in ROS scavenging [9,10]. It has been suggested that NADPH oxidase (NOX)-derived superoxide ($O_2^{\bullet-}$) controls, at physiological concentration, cell expansion during the apical growth of pollen tubes and that it local-izes in the apical region of these cells [23]. Moreover, there is a correlation between ROS and Ca^{2+} signaling, that is also essential for plant development and tip-growth, since ROS induce Ca^{2+} influx across cell membranes [24], and cytosolic Ca^{2+} can activate NOX; establishing a positive feedback between NOX activity and ROS-induced Ca^{2+} influx, that supports polarized growth [25]. Moreover, to avoid an excess of ROS that could lead to oxidative damage, pollen has a powerful antioxidant machinery based on superox-ide dismutase (SOD) that catalyzes the dismutation of $O_2^{\bullet-}$ into H_2O_2; the latter is decomposed to water and oxygen by catalase (CAT).

However, details on the reciprocal interactions between these factors are missing. In fact, although many cellular targets of PAs have been described, the precise molecular mechanisms of these interactions are largely unknown and the readily inter-conversion; oxidation and conjugation of PA complicate studies on the functions of the individual PA.

Since natural PAs are rapidly metabolized in cells, substituting the natural PA with analogs offers means to study either the function of an individual PA or the effect of modified PA metabolism on cell physiology. For example, the insertion of one or two aromatic rings on the terminal primary amino groups of natural PAs, could modify the hydrophilicity of the molecule, the rate of protonation of amine groups and their interaction with anionic counterpart of bio-logical molecules or the affinity toward enzymes. For this reason, the search for new PA analogs with physiological activity results to be a promising research field. In particular, our research has been focused on the assessment of the effect of natural and syn-thetic PAs on the apical growth of pollen tubes. Further, the present study aimed to understand if and how PAs and ROS concentration are interconnected in the process of tip-growth. Preliminarily, the effect on germinating pollen tubes caused by the natural PAs Cad, Put, Spd and Spm was assessed. Finding Spm as the most effective, besides natural PAs, symmetrically or asymmetrically substituted Spm, bearing different aromatic groups on one or both terminal amines were examined. The aromatic rings were chosen for their different electronic and/or lipophilic properties in order to evaluate any favorable effect on Spm activity. To this aim, we selected three synthetic Spm analogs, BD6, BD26, and BD23, substituted on one of the terminal primary amino group of Spm with a different aro-matic or heteroaromatic moiety such as benzyl, naphthalene, and pyridine, respectively. Spm analogs DL5 and DL6 were also selected due to the presence in their structure of the aromatic ring of vanillin, which is a natural compound endowed with antioxidant properties. Finally, three synthetic tetramines (Met 6-5-6, Met 6-10-6 and Met 5-10-5) related to methoctramine (Met 6-8-6), a M_2-muscarinic

receptor competitive antagonist [26], were also included in this study. These synthetic PAs, characterized by longer polymethylene chains than Spm and a 2-methoxybenzyl group on each terminal nitrogen atom, are able to bind a variety of receptor sites [27] and here were chosen due to their NMDA channel blocking activity [28]. In fact, NMDA receptor is involved in the Ca^{2+} ions trafficking in mammalians [28] and presents homologues in plants, where these glutamate-gated cationic channels, selective for Na^+, K^+, and Ca^{2+} ions, are involved in the plant immune response [29].

Our results show how important ROS are during pollen germination and that a link between PAs and ROS exists. Moreover, a slight imbalance in the two molecules was demonstrated to be detrimental and to drive the pollen toward a cell death.

2. Materials and methods

2.1. Chemicals

All chemicals (unless otherwise indicated) were obtained from Sigma–Aldrich (Milan, Italy).

2.2. Synthesis of substituted spermine analogs and methoctramine analogs

The synthetic PA analogs assayed in this study (Fig. 1), all in form of tetrahydrochloride salts, namely N^1-(3-aminopropyl)-N^4-(3-(benzylamino) propyl) butane-1,4-diamine or N^1-benzyl-spermine (BD6) [30], N^1-(3-aminopropyl)-N^4-(3-((pyridin-3-ylmethyl) amino) propyl) butane-1,4-diamine (BD23), N^1-(3-aminopropyl)-N^4-(3-((naphthalen-2-ylmethyl) amino) propyl) butane-1,4-diamine (BD26) [31], 4-(((3-((4-((3-aminopropyl) amino) butyl) amino propyl) amino) methyl)-2-methoxy phenol (DL5), 4,4′-(2,6,11,15-tetraazahexadecane-1,16-diyl) bis(2-methoxyphenol) (DL6) [32], N^1,$N^{1'}$-(pentane-1,5-diyl) bis(N^6-(2-methoxybenzyl) hexane-1,6-diamine) (Met 6-5-6), N^1,$N^{1'}$-(decane-1,10-diyl) bis(N^6-(2-methoxybenzyl) hexane-1,6-diamine) (Met 6-10-6) [26] and N^1,$N^{1'}$-(decane-1,10-diyl) bis(N^5-(2-methoxybenzyl) pentane-1,5-diamine) tetrahydrochloride (Met 5-10-5) [33], were synthesized as previously reported.

In particular, the mono-substituted Spm analogs BD6, BD23, BD26 and DL5 were synthesized by reacting tri-Boc-spermine with the appropriate aldehydes (1 eq. in Fig. 2) to afford the corresponding Schiff bases that were reduced in situ with $NaBH_4$. Acidic deprotection of the tri-Boc protected intermediates led to the corresponding tetraamines as tetrahydrochloride salts. The disubstituted Spm analog DL6 was obtained by reaction of Spm with 2-methoxybenzaldehyde (2 eq. in Fig. 2) followed by reduction of the Schiff base with $NaBH_4$.

The methoctramine analogs Met 6-5-6, Met 6-10-6 and Met 5-10-5 have been synthesized following the procedure developed by our research group. As example, the synthesis of compound Met 6-5-6 is reported in Fig. 2. Briefly, N-[(benzyloxy) carbonyl]-6-aminocaproic acid was reacted with 1,5-diaminopentane to give the intermediate 1; removal of the N-(benzyloxy) carbonyl group by acidic hydrolysis gave the corresponding diamine diamide 2, which was reacted with 2-methoxybenzaldehyde and then reduced with $NaBH_4$, to furnish derivative 3; reduction of 3 with BACH-EI (borane N-ethyl-N-isopropyl-aniline complex) in dry diglyme led to the desired tetramine Met 6-5-6.

2.3. Plant material

Mature pollen of pear (*Pyrus communis* cv. Williams) was collected from plants grown in experimental plots at the University of Bologna (Dipartimento di Scienze Agrarie, Università di Bologna).

Spermine analogues
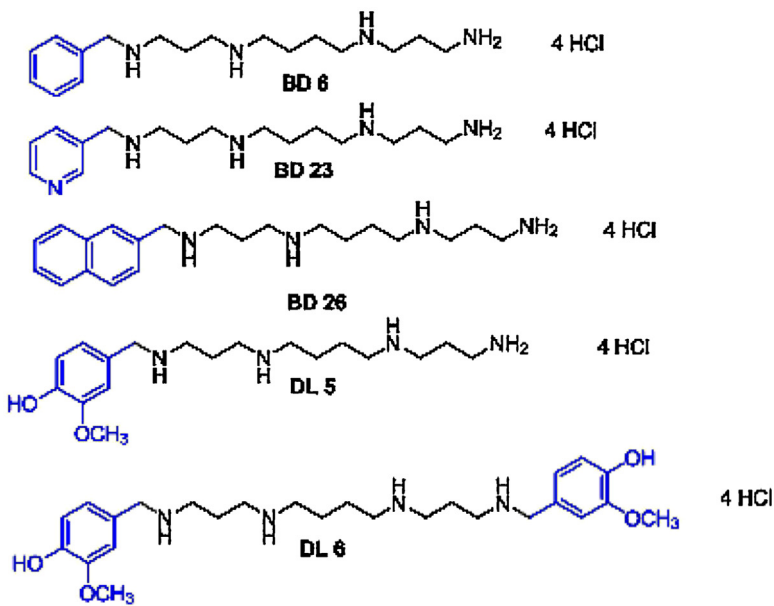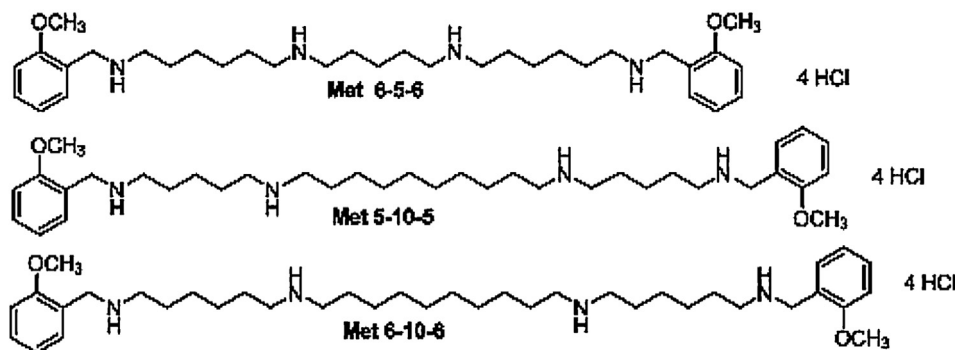

Methoctramine analogues

Fig. 1. PA analogs. In blue the structural components of the molecules different from those of spermine. (For interpretation of the references to color in this figure legend, the reader is referred to the web version of this article.)

Handling, storage, pollen hydration and germination were performed as previously reported [16,34]. After 1 h of growth, the medium was supplemented with different concentrations of PAs (Cad, Put, Spd or Spm), PAs analogs (BD6, BD26, BD23, DL5, DL6, Met 6-10-6, Met 5-10-5, and Met 6-5-6) or diphenyleneiodonium chloride (DPI) up to 2 h unless otherwise indicated. Pollen was visualized under a light microscope (Nikon Eclipse E600) equipped with

a digital camera (Nikon DXM1200). For growth recovery experiment, pollen was treated at different times with Spm and BD23 (100 and 500 μM) and then repeatedly washed with germination medium and allowed to germinate again. Recovery was calculated as mean pollen tube length after 2 h in comparison to the mean pollen tube length after the first hour of germination.
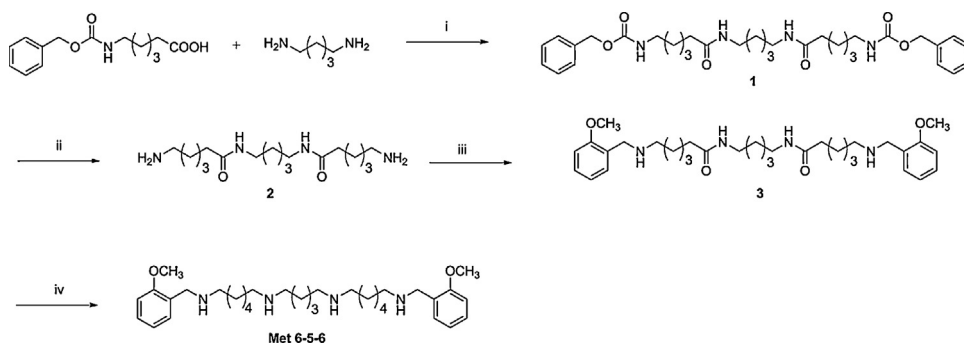

Fig. 2. Synthesis of compound Met 6-5-6. (i) EtOCOCl, NEt$_3$, dioxane, room temp., 18 h, 84%; (ii) a) HBr 33% in CH$_3$COOH, room temp., 4 h, quantitative yield; b) 2N NaOH, CHCl$_3$, 14 h; (iii) a) 2-methoxybenzaldheyde, MeOH; b) NaBH$_4$, EtOH, room temp., overnight, 90%; (iv) BACH-EI, diglyme, reflux, 12 h, 36%.

2.4. NAD(P)H-oxidase, catalase and superoxide dismutase in gel activity assay

Aliquots of germinating pollen were taken at different times during germination and PAs treatment then centrifuged for 3 min at $5000 \times g$, $4\,^{\circ}C$. Pelleted pollen was resuspended in 1 ml PBS 150 mM, pH 7.5, sonicated twice on ice for 15 s and centrifuged for 25 min at $5000 \times g$, $4\,^{\circ}C$. Protein concentration in the supernatant was analyzed by the bicinchoninic acid (BCA) assay kit. Freshly prepared extracts were separated in 12% to check SOD activity or 8% to check the NADP(H)-Ox and CAT activity (w/v) native-PAGE gels and visualized according to [35,36] with minor modifications. All protein in-gel activity assays were performed at least three times in order to ensure the consistency of results.

2.5. Calcium distribution

Ca^{2+} fluorescence was measured after chlortetracycline (CTC) addition and incubation for 2 min. The optimal concentration of CTC, that did not affect pollen growth but still provided good fluorescence signal, was determined to be about 100 μM. Samples were observed under a fluorescence microscope [Nikon Eclipse E600] using a proper filter.

2.6. ROS localization and spectrophotometric NBT assay

ROS detection using the fluorescent ROS indicator dye 2′,7′-dichlorodihydrofluorescein diacetate (DCFH$_2$-DA; Molecular Probes) was performed according to literature [37]. For nitroblue tetrazolium (NBT) staining, after 1 h of pollen germination, NBT was mixed with germination medium (final concentration 1.2 mM) and incubated for 10 min at room temperature. The staining due to formazan deposits was immediately visualized under a light microscope. The 3,3′-Diaminobenzidine (DAB) staining was performed as described in Ref. [38], with few modification. ROS quantification by absorbance of NBT color by spectrophotometric assay was performed as described in Ref. [39] with few modifications. Briefly, germinated pollen grains (1 mg/assay) were mixed with 2 mM nitroblue tetrazolium (NBT) and 1 mM nicotinamide adenine dinucleotide phosphate (reduced) (NADH). Negative controls were performed adding diphenyleneiodonium chloride (DPI) at final concentration of 100 and 200 μM. The reaction was conducted at $37\,^{\circ}C$ for 30 min, then the suspensions were centrifuged for 3 min at $10,620 \times g$. Residual non-reduced NBT was removed by washing with 1 ml of pure water twice. The formazan sediment was dissolved in 400 μl of methanol by shacking for 20 min at room temperature. After extraction, the suspensions were centrifuged for 3 min at $10,620 \times g$ and the absorbance of supernatants was measured at 530 nm.

2.7. Conjugation of spermine with fluorescein isothiocyanate (FITC) and Spm-FITC localization

The conjugation of Spm with fluorescein isothiocyanate (FITC) was performed using the FluoroTag FITC Conjugation Kit, according to the manufacturer instructions. A volume of 300 μl of the pollen suspension was supplemented with FITC-conjugated Spm in the dark. After 10 and 30 min, the suspension was centrifuged for 1 min at $180 \times g$ and the germination medium was replaced by an equal volume of BSA 3% (w/v) in PBS, pH 7.4. After 1-h incubation at $37\,^{\circ}C$, residual FITC-conjugated Spm was removed by washing with 200 μl of PBS, pH 7.4. Pollen was thus fixed with 200 μl methanol for 10 min at $-20\,^{\circ}C$. After fixation, pollen was washed, resuspended in 100 μl PBS, pH 7.4 and immediately visualized under a fluorescence microscope [Nikon Eclipse E600] adjusted at 488 nm for fluorescein excitation.

2.8. Pollen viability assay

To determine pollen viability MTT (2,5-diphenyl tetrazolium bromide) test was used. MTT produces a yellowish solution that is converted to dark blue, water-insoluble MTT formazan by mitochondrial dehydrogenases of living cells. The test solution contained a 1% concentration of the MTT substrate in 5% sucrose. After 15 min incubation at $30\,^{\circ}C$ the pollen samples were visualized under a light microscope. Only germinated pollen was taken into consideration as PAs were supplemented after the first hour germination. Germinated pollen was considered viable if it turned deep purple. At least 60 pollen tubes were observed per treatment, and each treatment was repeated three times in order to ensure the consistency of results. The percentage of viability was normalized on the control samples.

2.9. Preparation of pollen DNA and 4′,6-diamidino-2-phenylindole (DAPI) staining

100 mg of germinated pollen was pulverized with liquid nitrogen to a fine powder and DNA was extracted following CTAB-based protocol as described in Ref. [40] with minor modifications. The purity and concentration of the extracted DNA were evaluated by measuring the absorbance at 260 and 280 nm using a NanoDrop Spectrophotometer ND-1000 (EuroClone S.p.A., Italy). Five μg of extracted DNA was checked by electrophoresis on a 1.2% agarose gel and stained with gel red (Biotium). For DAPI staining, germinated pollen was fixed in 1.5% formaldehyde for 20 min, and then collected by centrifugation, 30 s at $1500 \times g$ at room temperature. The pollen was resuspended in pollen isolation buffer [100 mM Na_2HPO_4, pH 7.5; 1 mM EDTA; 0.1% (v/v) Triton X-100] and DAPI was added at final concentration 1 $\mu g/ml$. Samples were observed under a fluorescence microscope [Nikon Eclipse E600] using a DAPI filter.

2.10. Data and statistics

Pollen tube length, in gel-activity bands intensity, ROS and fluorescence distribution analysis, nuclear condensation and distance between vegetative and generative nuclei have been performed using ImageJ software. Differences between sample sets were determined by analysis of variance (two-way and one-way ANOVA, with a threshold P-value of 0.05) using GraphPad Prism.

3. Results

3.1. Exogenous PA supply effects on pollen tube elongation

To check the effect of natural PAs on germinating pollen tubes, the length of *P. communis* pollen tubes was measured after addition of different concentrations of Cad, Put, Spd and Spm, after the first hour of germination; treatment of pollen continued for an additional hour then the pollen tube length was measured. The length of control pollen tubes was on average 317 μm after the first hour of germination, but this average value rose to 1021 μm after the second one (Fig. 3). All the natural PAs, except Cad, were effective on pollen tube elongation in a dose-dependent manner. The most effective was Spm that drastically reduced by 46.32% pollen tube elongation at 10 μM and completely abolished it at 100 μM. In addition, Spd was quite effective, with an inhibition by 35.91% and 43.27% at 100 μM and 250 μM respectively, whereas Put showed a drop of pollen tube elongation by 51.36% and 58.32% only at final concentration of 750 μM and 1 mM respectively; the last value determined the arrest of pollen tube growth (Fig. 3).

Given that ROS are essential for pollen tube elongation and that exogenous PA supplementation blocked this process, the next
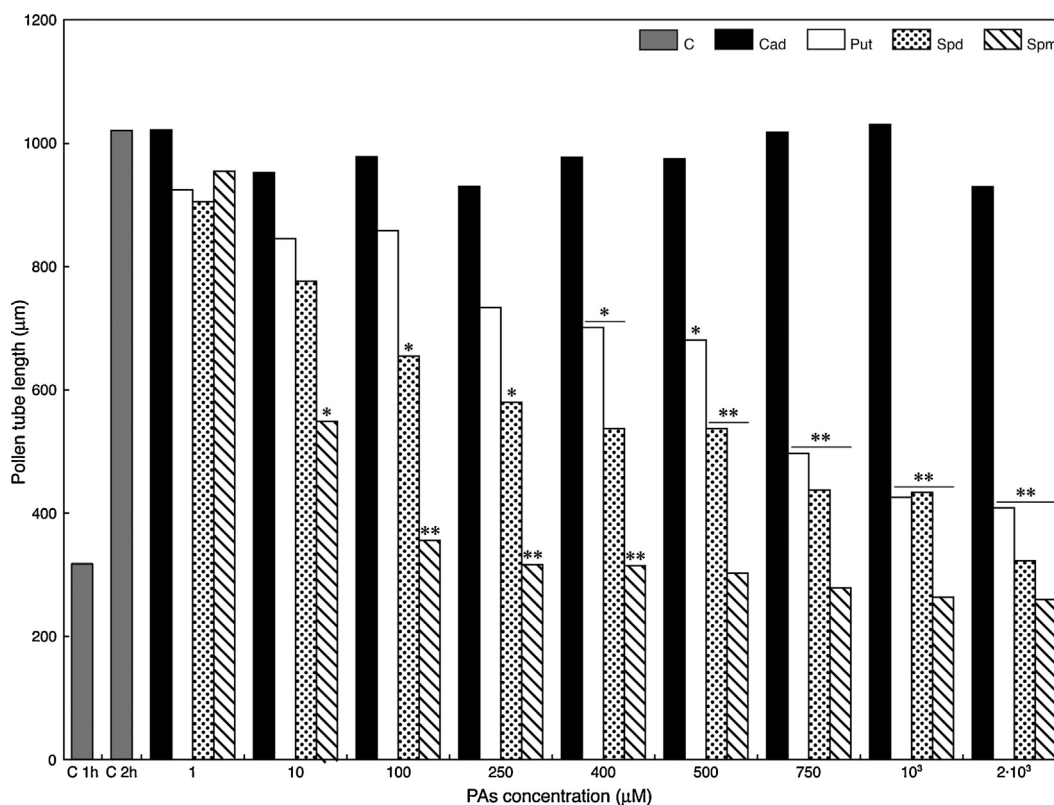
Fig. 3. Effect of Spm, Spd, Put and Cad on the elongation of pollen tube of *Pyrus communis*. Means derive from at least 40 measurements and the experiment was repeated three times. Means of treated samples were compared with control sample after 2 h germination by Dunnett's Multiple Comparison Test $^* = p \leq 0.05$; $^{**} = p \leq 0.01$. SD < 0.15.

goal was to understand if ROS and PAs localize in the same region of the pollen tube. Pollen cultures were incubated with the cell-permeable probe DCFH$_2$-DA and the fluorescence due to ROS presence was monitored over time after PAs supplementation. Staining with DCFH$_2$-DA revealed a tip-localized pattern of fluorescence in control tubes after 60 min germination (Fig. 4A a–c).

To monitor ROS formation over time, the incubation with PAs was split in time spans. After the first hour incubation PAs were supplied (100 μM) and within the first 10 min after PAs supplementation (70 min germination), the scenario was different from the control as the fluorescence intensity was less localized at the tip (Fig. 4A d–f). After 10–15 min from PAs supplementation swollen tips became evident and variability in the localization of the sig-nal occurred as it was diffused and very faint or localized in spots (Fig. 4A g–h). After 20 min treatment (70 min germination), the pollen tips assumed a lollipop-shape and the same heterogeneity observed before was again evident (Fig 4A i–l), with in addition some tips having newly tip-localized ROS (Fig. 4A m).

3.2. Localization of Spm-FITC and ROS in the pollen tube

Once established that the concentration of ROS is higher in the apical region of pollen tubes and that the supply of exogenous PAs affected ROS gradient, the entry site of PAs and their distribution in pollen tubes were checked to determine if PAs co-localize with ROS. For this purpose, labeling of Spm by conjugation with fluorescein isothiocyanate (FITC) was performed (Fig. 4B). Grain showed strong auto-fluorescence but fluorescence due to the labeled Spm was clearly detectable and showed that it entered and localized at the pollen tube tip region within 10 min after PA supply (Fig 4B a and b), then diffused and localized in the apical and sub-apical regions, according to a gradient profile with maximum concentration at the tip (Fig. 4B c and d).

Fluorescence-intensity distribution analysis has been performed to understand if PAs and ROS localize in the same region of the pollen tube. ROS in non-treated pollen (Fig. 4C, gray line) are distributed within the first 200 μm of pollen tubes with its maximum at 30 μm. The same ROS concentration profile is present if pollen is treated with 1 μM Spm (Fig. 4C, blue line). After treatment with 100 μM Spm (Fig. 4C black line) pollen tubes were drastically inhibited and the ROS gradient was undetectable. The distribution of the ROS gradient reflected the distribution of FITC-conjugated Spm (Fig. 4C, green line), that also blocked pollen tube elongation and showed a distribution with higher concentration within the first 100 μm, exactly in the same zone of ROS localization (Fig. 4C).

3.3. Effects of synthetic PAs on pollen tube elongation

Since Spm was found to be the most effective among the aliphatic PAs, different Spm analogs have been tested. Four of them, BD26, BD6, DL5, and BD23 are Spm analogs asymmetrically substituted on one of the terminal amine functions with different aromatic groups, while DL6 bears a 2-methoxybenzyl group on each terminal nitrogen atoms of Spm. DL5 and DL6 were selected for the presence in their structure of the aromatic ring of vanillin, which is a natural compound endowed with antioxidant properties. In addition, three synthetic tetramines (Met 6-5-6, Met 6-10-6 and Met 5-10-5) related to methoctramine and characterized by a longer polymethylene chain (when compared to Spm) and a 2-methoxybenzyl group on each terminal nitrogen atoms, were included in the study (Fig. 1). Likewise to the experiment performed with natural aliphatic PAs, we supplemented the pollen germination medium with the different Spm and Met 6-8-6 analogs. All the synthetic PAs were effective on pollen tube elongation in a dose-dependent manner. Among the PAs mono-substituted on one-terminal primary amino group, the most effective was BD23,
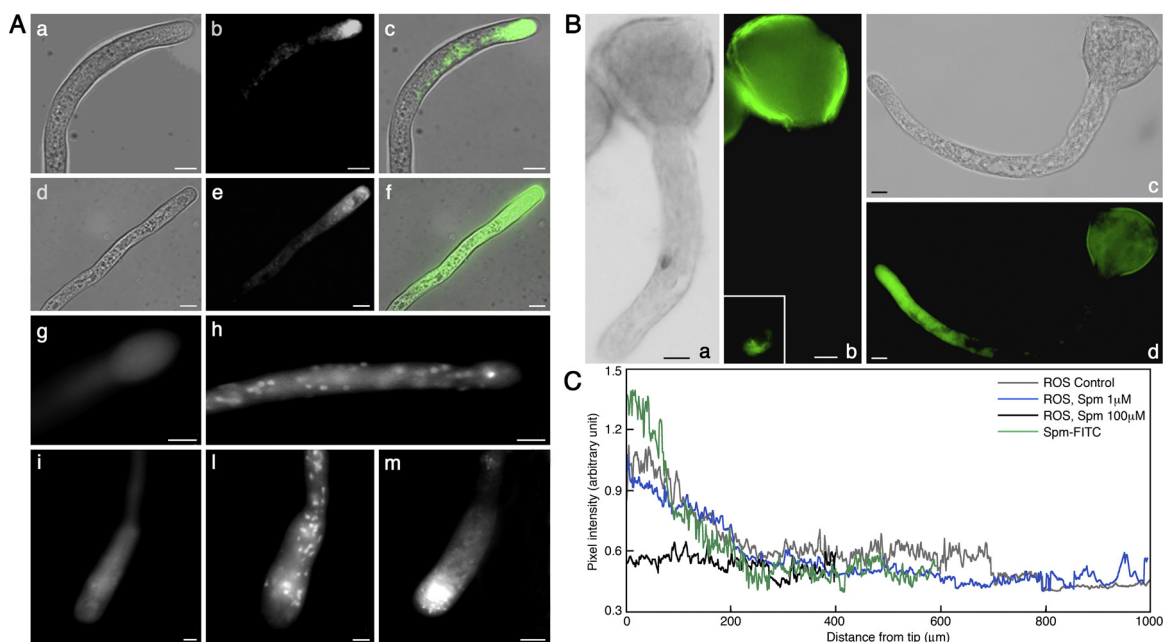
Fig. 4. Spm co-localizes with ROS in germinating pollen and affects ROS distribution. (A) Tip-localized fluorescence due to the ROS probe DCFH2-DA (a–c) is slightly decreased within 10 min after PAs supplementation (d–f). Variability in the localization of the signal after 11–16 min treatment are shown in g and h, where fluorescence is diffused and faint or localized in spots (g and h respectively). After 20 min treatment the heterogeneity in ROS localization is still evident (i and l), with in addition some tips having newly tip-localized ROS (m). (B) FITC-labeled Spm localization in the pollen tube after 10 min supplementation (a and b) and 30 min supplementation (c and d). Bars = 10 μm. (C) Line graph with the distribution of ROS in control pollen (gray line) and in pollen treated with Spm 1 and 100 μM (blue and black lines respectively) in comparison to the distribution of FITC-Spm after 30 min incubation.

which drastically reduced by 69.27% pollen tube elongation at 100 μM, namely less efficiently than Spm.

A similar pattern was observed for DL5, characterized by a different aromatic moiety (a vanillyl group in DL5 vs. a 3-pyridyl moiety in BD23). BD26 was also quite effective, with an inhibition by 54.77% and 71.38% at 100 μM and 250 μM respectively, whereas BD6 caused the arrest of pollen tube growth only at higher concentrations, with a drop of pollen tube elongation by 59.41% at 750 μM (Fig. 5A).

All the di-substituted PAs (DL6, Met 6-5-6, Met 6-10-6 and Met 5-10-5) were effective only at a final concentration of 100 μM (or higher than 100 μM) and the most effective was Met 6-5-6, that reduced by 65.72% pollen tube elongation at the concentration of 100 μM. Met 6-5-6, Met 5-10-5 and Met 6-10-6 decreased pollen tube elongation on average by 74% at concentration of 250 μM while DL6, characterized by two vanillyl moieties, displayed the same effect only at 500 μM (Fig. 5B).

3.4. Effects on tube morphology and growth recovery of pollen tube after Spm or BD23 treatments

Since Spm and its 3-pyridyl derivative BD23 were the two most effective PAs among the natural and synthetic PAs, respectively, they were used to perform the following experiments. Moreover, one hour-incubation with 100 μM of Spm and BD23 not only abolished pollen tube elongation, but also caused the swelling of the apex. This morphological change increased when concentrations higher than 100 μM of both PAs were supplied; higher concentrations induced a "lollipop-shape" of the apical region (Fig. 6A). As demonstrated by a time-course experiment, supplementing the growing medium with 500 μM Spm and BD23 induced an enlargement of the apical region in some pollen tubes after 10 min but the swelling became a permanent feature after 15 min and was more evident after extended incubations (Fig. 6B).

We performed a growth recovery assay to understand if the removal of PAs from the medium might allow pollen tubes to recover growth. The average recovery from Spm and BD23 effects was affected by both duration of treatment and concentration of PAs (as shown in Table 1). No complete recovery was detected but a time-dependent trend was observed when pollen was treated with 100 μM of Spm and BD23. In fact, more than 32% recovery of growth rate occurred after 5 min of PAs treatment (36.17% for Spm and 32.92% for BD23); this rate gradually decreased to around 24% after 10 min (23.8% for Spm and 29.91% for BD23) and to 15% on average after 20 min treatment (18.97 for Spm and 12.03% for BD23). No recovery was observed for longer incubation with the two PAs. More drastic was the effect of treatment with 500 μM PAs that allowed a little recovery just after 5 min treatment with a recovery rate of 26.52% and 18.21% for Spm and BD23, respectively.

3.5. Spm and BD23 effect on $O_2^{\bullet-}$ and H_2O_2 concentration

The overall decrease of tip-localized ROS after PAs treatment was confirmed by using two compounds that are specific for two types of ROS: NBT and 3,3′-DAB. In fact, the capacity of NBT to be reduced by $O_2^{\bullet-}$ and to form intense purple formazan deposits was evaluated. After 10 min of incubation with NBT, one hour-germinated pollens showed formazan deposits (Fig. 7A). The staining was much more intense in the tip domain, but it also extended for several micrometers (40–60 μm in mean) backwards. Formazan deposits were detectable in the same zones after pollen treatment with 1 μM Spm and BD23. In contrast, NBT reduction in the apical zone was completely abolished in pollen tubes treated with 100 μM Spm and BD23. In addition, pollen treated with the NOX inhibitor diphenylene iodonium (DPI), which prevents the production of $O_2^{\bullet-}$, showed no formazan deposits. This result is consistent with the possible activity of NOX as the source of ROS production, essential for pollen tube tip-growth (Fig. 7A).

Detection of H_2O_2 by DAB staining showed dark brown precipitates diffusely present along the entire pollen tubes not treated with PAs. In contrast, formation of precipitates was completely abolished in the apical zone when treated with Spm or with BD23 at 100 μM,
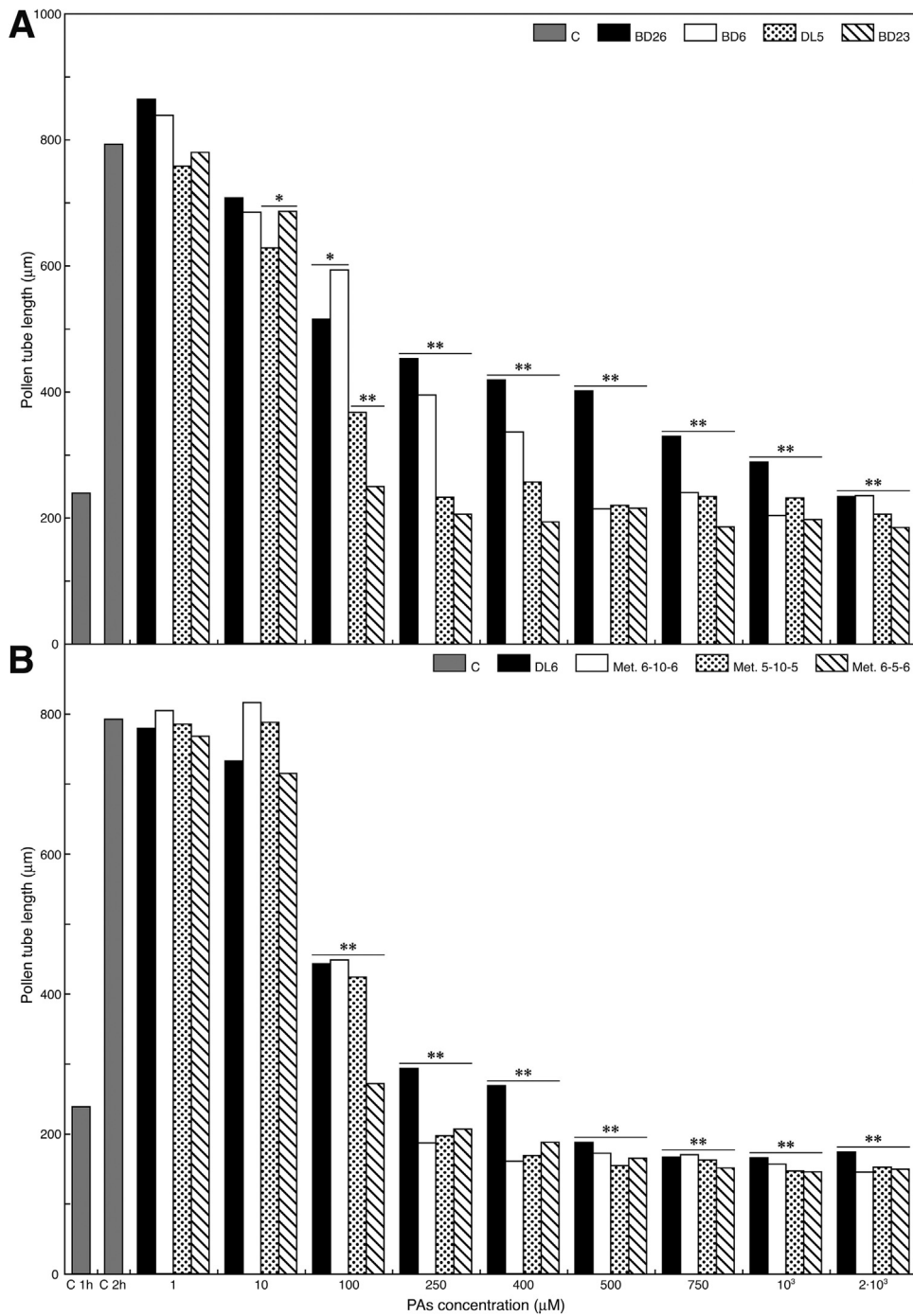
Fig. 5. Pollen tube length after treatment with different concentration of Spm-analogs. (A) Effect of synthetic PAs with a primary terminal amino group on pollen tube elongation; (B) Effect of the synthetic PAs with no primary terminal amino group. Means derive from at least 40 measurements and the experiment was repeated three times. Means of treated samples were compared with control sample after 2 h germination by Dunnett's Multiple Comparison Test. $^* = p \le 0.05$; $^{**} = p \le 0.01$. SD < 0.15.

Table 1

Recovery experiment after PAs supplementation. Recovery is expressed, in percentage, as mean of pollen tube length after Spm and BD23 treatment for different times, in comparison to control samples.

	100 μM				500 μM			
	5 min	10 min	20 min	45 min	5 min	10 min	20 min	45 min
Spm Recovery	36.17 ± 7.91	23.8 ± 6.14	18.97 ± 6.85	–	26.52 ± 5.9	–	–	–
BD23 Recovery	32.92 ± 7.8	29.91 ± 8.01	12.03 ± 8.27	–	18.21 ± 6.4	–	–	–

Means derive from at least 60 measurements and the experiment was repeated three times. Means of treated samples were compared with control sample after 1 h germination by Dunnett's Multiple Comparison Test. All values reported are statistically significant ($p \le 0.01$, SD < 0.15).
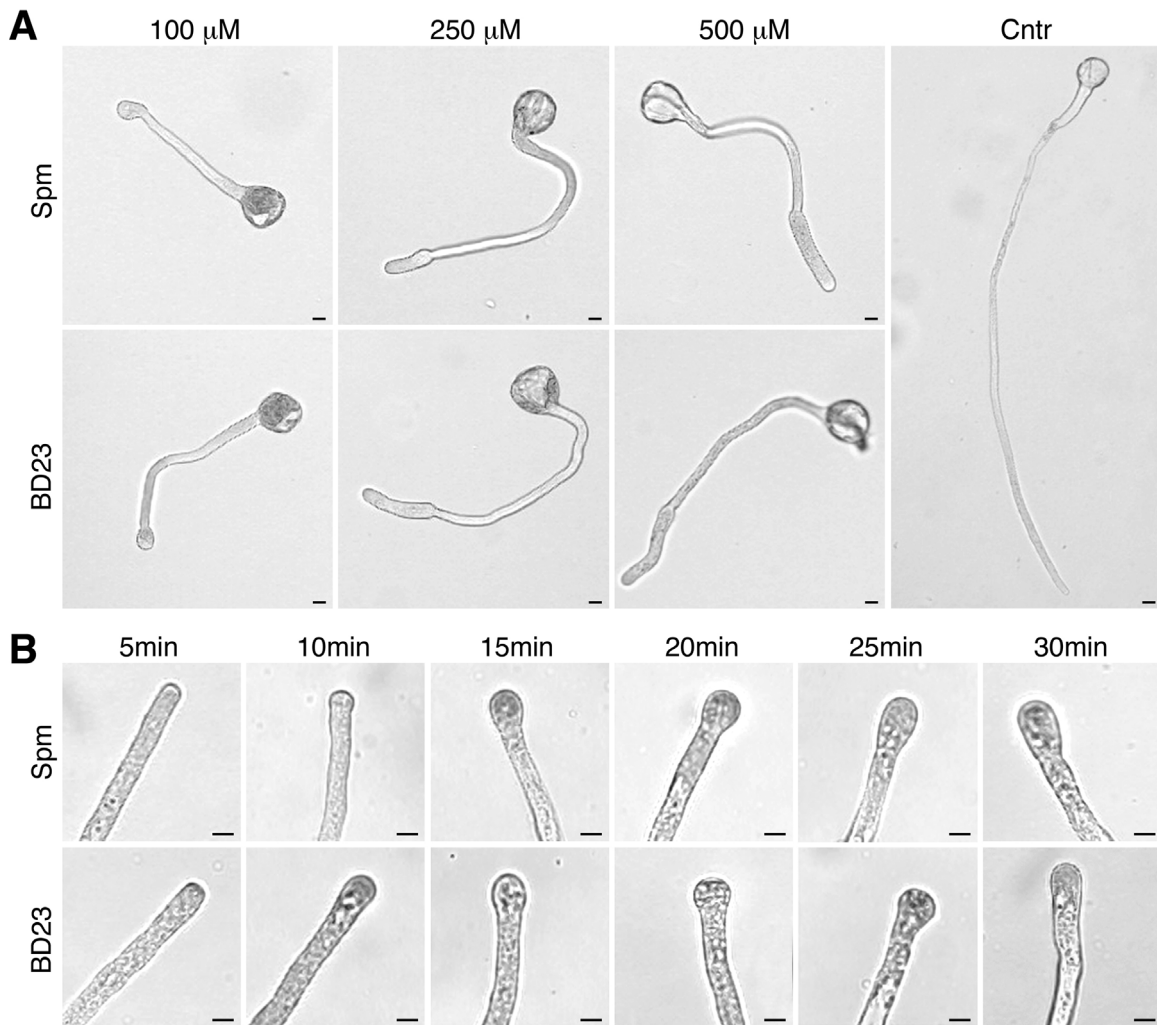
Fig. 6. Morphological changes in pollen tubes treated with different concentration of Spm and BD23. (A) Dose-dependent swelling of the pollen tube tip after treatment with Spm and BD23 in comparison to a control pollen tube. (B) Time-lapse swelling of the pollen tube tip after addition of Spm and BD23 500 μM. Bars = 10 μm.

whereas at 500 μM Spm had a stronger and more diffused effect (Fig. 7B).

To measure the relative levels of endogenous ROS in both germinated control and PAs treated pollen, we performed a ROS quantification using NBT and, in particular, by measuring the absorbance of the purple formazan sediment (Fig. 7C). The NBT-reducing activity was enhanced by the addition of NADH thus suggesting that it was due to the generation of ROS by pollen NOX. Both Spm and BD23 at 100 μM nearly completely inhibit the formation of formazan sediments. A similar result was obtained when pollen was treated with 200 μM DPI, whereas 100 μM concentration had a significantly lower inhibiting effect (Fig. 7C).

To check the precise concentration of both Spm and BD23 that inhibits ROS formation, a dose dependent-experiment has been performed (Fig. 7D). 10 μM Spm very slightly decreased ROS-mediated NBT reduction, while its analog BD23 was not effective at the same concentration. A drastic decrease of formazan production was clear for both PAs at 50 μM, in fact Spm and BD23 decreased NBT reduction by 51.2% and 70.5% respectively, whereas at 100 μM, the absorbance of the formazan fall down to background levels, with a final drop of NBT reduction by 78.5% and 90.1%, respectively, for Spm and BD23 (Fig. 7D).

3.6. Ca^{2+} gradient alteration and effect on NOX enzyme activity by Spm and BD23

It is well known that PAs play also a role in modulating Ca^{2+} signaling and that Ca^{2+} gradient and the tip-localized Ca^{2+} influx play a pivotal role in the apical growth of pollen tubes also in relation to ROS production [25,41]. We decided to investigate if/how exogenous PAs supplementation could affect the tip-focused intracellular Ca^{2+} gradient, since the above-mentioned results showed that PAs affect pollen tube morphology. Fig. 8A shows that the tip-focused Ca^{2+} gradient was drastically altered within 2–10 min after addition of PAs as Ca^{2+} distribution was less focused at the tip and more diffused in the sub-apical region of the pollen tube. The Ca^{2+} gradient was restored during the formation of the swollen apex, when it became tip-localized again.

Considering that PAs affect ROS and Ca^{2+} distribution and that NOX enzymes are sensitively affected by Ca^{2+} perturbations, the activity of the O$_2$$^{\bullet-}$ producing enzyme was investigated. The two PAs induced a sudden but short-lasting stimulation in the activity of the enzyme. In particular, both Spm and less significantly BD23 increased the activity of the enzyme by 130–150% within the first 2–5 min treatment but their effects were not detectable for times longer than 15 min (Fig. 8B).
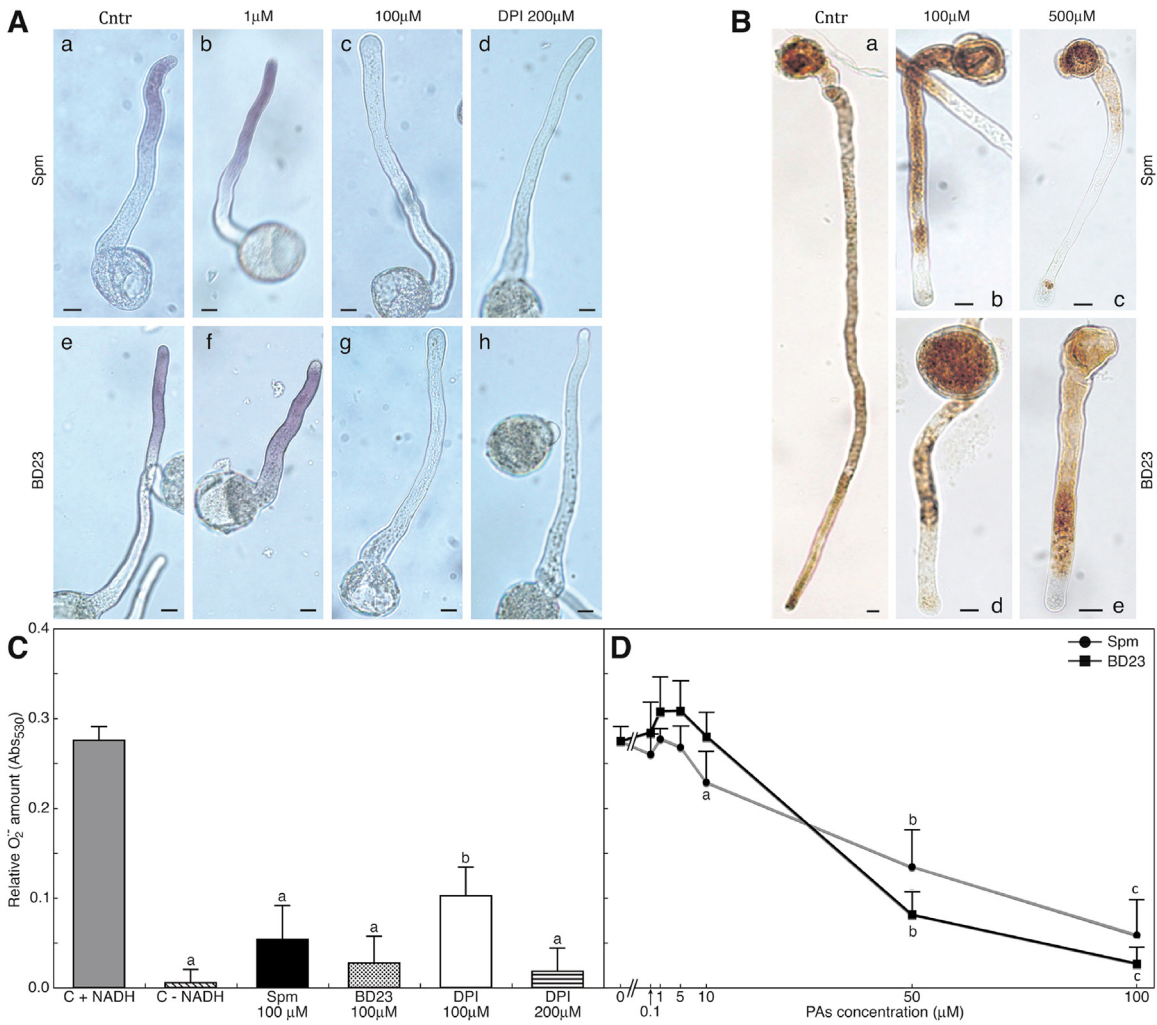
Fig. 7. Spm and the Spm-analog BD23 decrease ROS concentration in germinating pollen. (A) $O_2^{\bullet-}$ distribution in control pollen and in pollen treated with Spm and BD23 1 and 100 μM. As negative control, pollen was treated with 200 μM of DPI, inhibitor of NOX. Bars = 10 μm. (B) H_2O_2 distribution in control pollen and in pollen treated with Spm and BD23 100 and 500 μM. Bars = 10 μm. (C) Relative amount of $O_2^{\bullet-}$ in pollen samples treated with Spm and BD23 100 μM in comparison to control samples. As negative control DPI 100 and 200 μM was used. Background is defined by a control sample not supplemented with NADH. Means derive from at least 12 measurements and the experiment was repeated four times. Means of treated samples were compared with control sample by Dunnett's Multiple Comparison Test. (D) Dose-dependent $O_2^{\bullet-}$ scavenging by Spm and BD23. Means derive from at least 12 measurements and the experiment was repeated four times. Means of treated samples were compared with control sample by Dunnett's Multiple Comparison Test.

3.7. Spm and BD23 effect on pollen antioxidant machinery

As the two PAs stimulate ROS production nearly instantly after supplementation, but ROS were generally decreased by both Spm and BD23, the next goal was to understand if pollen activates its antioxidant machinery in response to the exogenous PAs and NOX enzyme activation. Specific activities of the antioxidant enzymes SOD and CAT were measured. Gels for the SOD in-gel activity showed two major bands in the protein extracts of pear pollen, indicating the presence of two SOD isozymes (Fig. 9A). The two PAs induced changes in the activities of both SOD isozymes; in particular, Spm induced a drastic (by 250%) and long-lasting effect with enzyme-stimulation that persisted through the whole treatment. Conversely, BD23 affected the activity of the enzyme that was increased by 180% after 5 min treatment but the effect on both SOD isozymes was not notable for longer times (Fig. 9A).

CAT activity was also analyzed. CAT isozymes were not distinguished and only one large band was observed in all of the times assayed. CAT activity was also affected by the two PAs with a slight time-shift (10–15 min) in comparison to SOD activity. This enzyme was also differently affected by the two PAs, since Spm induced an almost steady increase for 30 min while CAT activity after BD23 treatment was rapidly decreased remaining lower than the controls at 40–60 min post-treatment (Fig. 9B).

3.8. Effect of Spm and BD23 on pollen viability, DNA and nuclei

To determine if the reduction of the apical pool of ROS might have detrimental effects, a time-course viability test was performed. The germination medium was supplemented with Spm or BD23 after the first hour of germination, and pollen viability was assessed using MTT (2,5-diphenyl tetrazolium bromide) staining. As comparison, DPI was also assayed. As shown in Fig. 10A, the two PAs, when supplemented at 100 μM, halved the viability of pollens after 50 min (110 min germination), while after 60 min incubation the viability drastically dropped by 21.1% and 24.5% for Spm and BD23, respectively (Fig. 10A). More effective was the treat-ment with 500 μM PAs, which halved the viability of pollens after 30-40 min with no viable pollens detected after 60 min (120 min germination). More drastic was the treatment with 100 μM DPI, whose supplementation in the germination medium halved the viability of pollens after only 10 min (Fig. 10A).
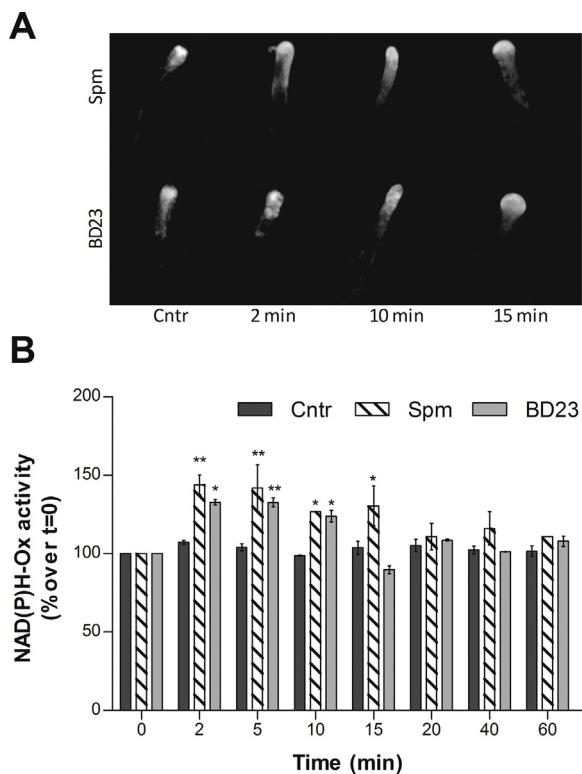
Fig. 8. Calcium distribution and NOX activity are altered by PAs supplementation. (A) Tip-localized fluorescence due to the Ca^{2+} probe CTC is completely dissipated after 2 and 10 min PAs supplementation. The gradient is restored after 15 min, when the swollen apex has formed. (B) Effect of Spm and BD23 on the NOX enzyme over time. Control samples ($t = 0$) were set as 100%. Means derive from at three independent experiments. Means of treated samples were compared with control by Dunnett's Multiple Comparison Test. $* = p \leq 0.05$; $** = p \leq 0.01$.

To test whether PAs-induced ROS-decrease could lead toward cell death, 60 min-germinated pollen was treated for additional time lapses with 500 μM Spm or BD23 and DNA fragmentation was assessed after different incubation times. Spm and BD23 stimulated DNA fragmentation after 30 min incubation, as demonstrated by DNA-laddering, while there were no evidences of DNA fragmentation in control pollen after 2 h germination. Incubation with 100 μM DPI induced DNA laddering after 15 min and the extent of fragmentation was significantly higher when compared with PAs (Fig. 10B). The sizes of DNA bands were approximately multiples of 200 bp, which is consistent with fragmentation at internucleosomal sites.

As the DNA degradation showed a large increase after PA treatment, the number and characteristics of nuclei in treated or untreated pollens was evaluated by the DNA fluorescent stain DAPI. Pollen tubes with two nuclei were regarded as normal, and the generative and vegetative nuclei were clearly distinguishable since the chromatin of generative cell nuclei was more highly condensed and more deeply stained with DAPI than that of vegetative nuclei. The complete absence of the two nuclei was observed as well as the presence of a single nucleus, suggesting that the vegeta-tive nucleus had degraded. As shown in Fig. 10C, treatment with 100 μM PAs decreased the percentage of bi-nucleated pollens and increased especially the number of pollens with one nucleus. Con-versely, treatment with 500 μ M PAs caused a drop in the number of bi- and mono-nucleated pollens, leading to a majority of pollens with no nucleus. In addition, the Ac-DEVD-CHO peptide (DEVD), an inhibitor of caspase-3, has been supplied to pollen to determine if it could reduce the process of DNA degradation. The degradation of nuclei was completely abolished when pollens were pre-treated with the DEVD peptide and then with PAs 100 μ M, while pre-treatment with DEVD could not completely counteract the effects of PAs supplemented at 500 μ M. In this case, only the number of mono-nucleated pollens increased, but not the number of bi-nucleated ones.
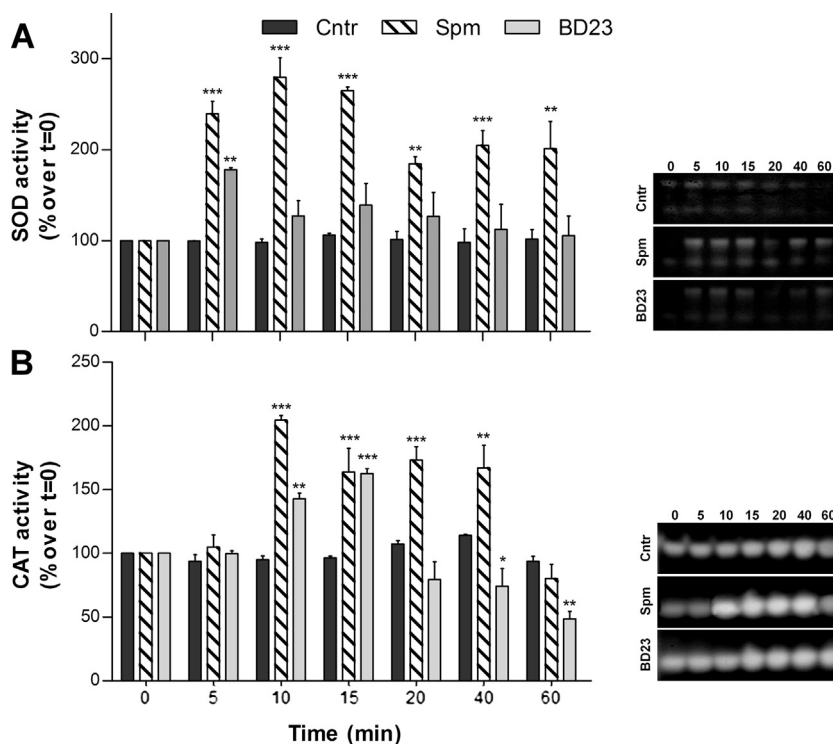
Fig. 9. Spm and BD23 stimulate the antioxidant machinery. Effect of Spm and BD23 on SOD (A) and CAT (B) enzymes over time. Control samples ($t = 0$) were set as 100%. Means derive from at three independent experiments. Means of treated samples were compared with control by Dunnett's Multiple Comparison Test. $* = p \leq 0.05$; $** = p \leq 0.01$; $*** = p \leq 0.001$. On the right of fig A and B, representative images of the in gel activity of both enzymes are shown.

Fig. 10. PAs induce DNA degradation and lead to cell death. (A) Time-dependent viability test after treatment with DPI 100 μM, Spm and BD23 100 and 500 μM. In each treatmen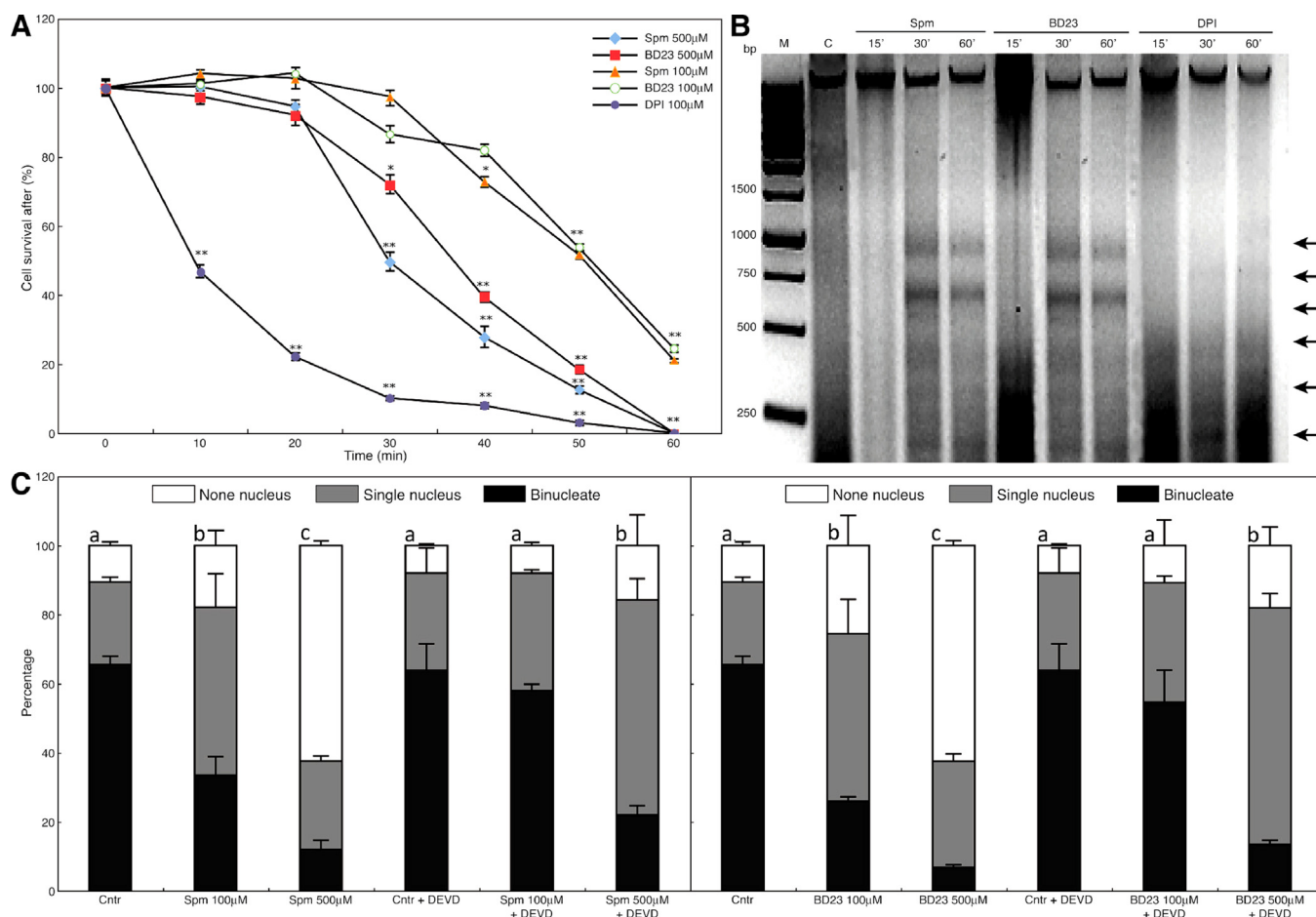t, at least 200 pollens were counted and the experiment was repeated twice. Means of treated samples were compared with control by Dunnett's Multiple Comparison Test. $^* = p \leq 0.05$; $^{**} = p \leq 0.01$. Results are normalized on control samples. (B) DPI 100 μM, Spm and BD23 500 μM induce DNA-laddering. (C) Rate of degradation of nuclear DNA after treatment with DPI, Spm or BD23 and inhibition of this process by the DEVD peptide, an inhibitor of caspase-3. In each treatment, at least 100 pollen tubes were counted and the experiment was repeated twice. Bars labeled by the same letter are not significantly different. Analysis of variance was performed by two-way ANOVA test, with Bonferroni post-test.

Treatment with 100 μM DPI drastically decreased the percentage of bi-nucleated pollens and increased especially the number of pollens with no nucleus in comparison to control pollens.

The pre-treatment with DEVD could counteract the effects of DPI and led to an increase in pollens showing only one nucleus.

Besides the preferentially degradation of the vegetative nucleus, treatment with 100 μM Spm and BD23 induced chromatin condensation in the generative nucleus, that resulted more intensely stained with DAPI (Fig. 11A and D) and smaller (Fig. 11B and D). Moreover, the two nuclei appeared more closed each other in respect to untreated control (Fig. 11C and D).

4. Discussion

Exogenous application of natural and synthetic PAs to the germination medium of *P. communis* pollen arrested the process of pollen tube elongation according to the concentration of PAs supplied. Spm was the most effective among the four natural PAs tested because it inhibited pollen growth from 10 μM onwards and modified the morphology of the apex, also leading toward cell death. The different natural PAs are effective according to the length of their backbone whereas the diamine Cad, demonstrated to enter the pollen tube [42], is without effect on pollen tube elongation according to the reported limited role of Cad in plants [43].

The effect of natural PAs has been also observed in other pollen from Rosaceae i.e., *Prunus dulcis*, in which the effect of Put, Spd and Spm has been shown to be dose-dependent thereby promoting pollen tube elongation at PAs concentrations up to 50 μM, whereas higher concentration resulted inhibitory for pollen tube elongation [44]. Furthermore, in *Actinidia deliciosa* high levels of PAs correlate with male sterility thereby causing reduced pollen development and tube growth [18,45]. The exogenously supplied Spd might modify the cell wall, as it is generally accepted that most of the cellular Spd pool is localized to the cell wall compartment [46], including the pollen cell wall in the form of hydroxycinnamic acid amides [47].

Plants are known to produce a complex mixture of amide conjugates of the more common PAs with various phenolic acids, namely hydroxycinnamic acids, differing in numbers of hydroxyl and methoxyl groups. For example, presence of hydroxycinnamoyl-Spd was linked to pollen grain development in Arabidopsis [47]. Although some of the PAs assayed in the present study contain hydroxy- and/or methoxy-substituted aromatic rings, the substitution performed on the terminal amine function preserves its basicity. Thus, all the molecules maintain the tetracationic form as Spm at physiological conditions and are not amide derivatives. Moreover, the focus here was just to determine the effects of Spm and its aromatic analogs on pollen tube growth.
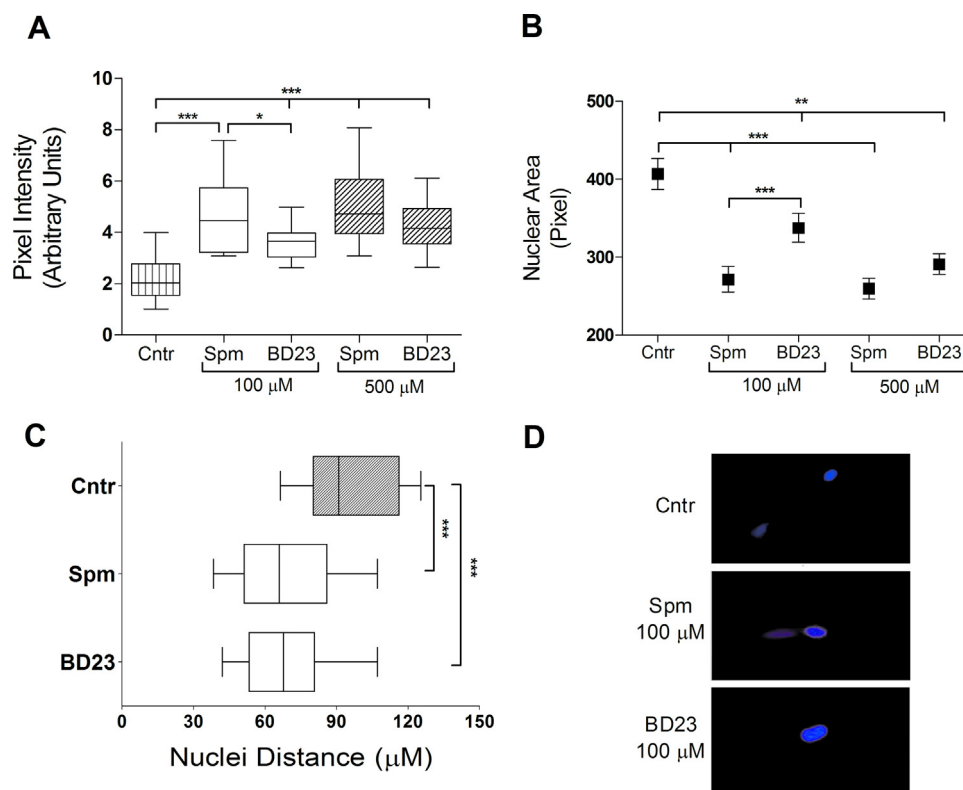
Fig. 11. PAs induce nuclear alterations. (A) Dose-dependent nuclear intensity and (B) nuclear condensation after treatment with Spm and BD23 100 and 500 μM. In each treatment, at least 30 nuclei were counted and the experiment was repeated twice. (C) Distance between vegetative and generative nuclei in control pollens and after treatment with Spm and BD23 100 μM. Means of treated samples were compared with control by Dunnett's Multiple Comparison Test. * = $p \leq 0.05$; ** = $p \leq 0.01$; *** = $p \leq 0.001$. (D) Nuclei stained with DAPI of control pollen showing the less condensed vegetative nucleus and the highly condensed generative nucleus. Treatment with 100 μM Spm and BD23 induced the preferentially degradation of the vegetative nucleus and caused chromatin condensation in the generative nucleus. Representative images were chosen.

Present data clarify that Spm also rapidly enters tube pollen tip and affects cytoplasmic and nuclear metabolism, thus not simply altering cell wall rebuilding. Spm then diffuses and localizes in the apical and sub-apical regions, according to a gradient profile with maximum concentration at the tip. Apical localization of PAs was also previously observed [42] and it was shown that these polycations are component of the pollen cell wall [3]. The swelling of the apex as well as its lollipop-shape clearly show that the cell wall is severely affected by the PA supplied. It was previously observed that PAs co-localized with TGase and are its substrates in vivo by conjugating one (mono-PA) or both (bis-PA) terminal aminic group/s of PAs to protein glutamyl residues. If a cross linkage is formed by bis-PA, proteins remain bound to each other forming a strong net that is no more degraded by proteases; if only mono-PA are formed, the net cannot be built or it is less strong, thus allowing swelling [3,6,48]. It was also shown that PAs are covalently bound via the enzyme TGase, to actin and tubulin and that at relatively high concentration they block the cytoskeleton-based movement [34,49]. These reports suggest that one of the possible mechanisms by which Spm and other aliphatic PAs arrested the germination of pollen tubes involves the cytoskeleton-based trafficking, which is essential for pollen tube growth and proper formation of the cell wall.

The reversibility of the growth inhibitory effect is only partial and decreased with time, thus the action of PAs is irreversible and increases in time. This evidence is in agreement with data that show that the linkage of PAs to the cytoskeleton proteins is irreversible, forming rigid actin bundle-like aggregates that cannot move further [49].
However, the effect of Spm seems to be even more complex, as in addition to the events possibly related to TGase-mediated

cell wall and cytoskeleton alteration, other events take place by involving ROS formation/scavenging and, finally, by affecting pollen viability. New data obtained with the present research highlight the co-localization of PAs with pollen tube ROS, as well as changes of different oxidative enzyme activities, showing that also the redox events are deeply and rapidly affected by PAs in the pollen tube. The same relationships between PAs and ROS have been sug-gested by literature data in other plant models [21,41,50]. ROS act up/downstream of various signaling cascades [51] and are essential during cell development and pollen tube elongation [20,52].

Present results clearly show that a large amount of ROS formation derives rapidly from pollen NOX activity as the NOX inhibitor DPI caused the disappearance of ROS along the tube apical region and inhibited pollen tube growth. Moreover, Spm suddenly stimulated NOX activity and thus ROS formation, also probably altering Ca^{2+} influx. NOX activity stimulation was followed by SOD and CAT activity increase, probably as consequence of the increased ROS production. It was suggested that PAs, except for Cad, could be involved in the plant defense mechanism by stimulating the antioxidant machinery and decreasing the oxidative stress intensity under water deficit conditions [53,54].

In addition, the eight synthetic PAs included in this study were shown to be effective, inhibiting pollen tube elongation from 100 μM onwards with the exception of DL5 and BD23 that showed inhibitory effect at 10 μM. Within the Spm-derivative series with one aryl-substituted primary amine group, the pattern of activity seemed to be related to the steric hindrance of the aryl group and to the presence of electron-donating groups on it. As results, BD23 was the most effective PAs, followed by DL5, BD6 and finally BD26, the latter characterized by the most bulky naphthalene ring. In general, the presence of two aromatic groups at both ends of the PA back-

bone caused a reduction in activity. As shown by comparing DL6 to DL5, which bear two and one vanillyl groups, respectively, at least one primary amine function is essential. The longer polymethylene tetramines (Met 6-5-6, Met 6-10-6 and Met 5-10-5) characterized by two 2-methoxybenzyl groups were also effective, but they did not cause a swollen tube tip, pointing out a different mechanism in the inhibition of pollen tube elongation. In a previous study it was found that these polymethylene tetramines act at different cellular levels, as they bind to DNA with a higher affinity than Spm and lead to oxidative stress [40].

In summary, the structure-activity relationships found in the present study indicates that the general activity of PA derivatives is tuned by: I) the presence or absence of one primary amino group, II) the steric hindrance of the aromatic group, III) the length of the carbon backbone and IV) the presence of hydrophilic and/or electron-donating groups on the aryl ring. All these evi-dences suggest that those compounds probably enter the cell, in accordance with their solubility and ability to pass through the plasma membrane. Moreover, recently, the L-type amino acid transporter (LAT) family transmembrane proteins have been iden-tified as transporters of both PAs and the herbicide paraquat (1,1′-Dimethyl-4,4′-bipyridinium dichloride) characterized by two quaternary ammonium cations. Arabidopsis LAT family proteins showed different subcellular localization properties (plasma mem-brane, Golgi and endoplasmic reticulum), which suggested that these transporters were involved in intracellular PA trafficking and PA uptake across the plasma membrane [55].

The pyridine Spm-derivative BD23 showed, even if at higher concentration, in many cases no significantly different effects from those of Spm, causing the arrest of tube elongation, changes in tip morphology, vitality, nuclei persistence, cell death, growth recov-ery, ROS gradient and H_2O_2 production. Further, SOD and CAT showed very similar activities but evidenced a more marked tran-sient enhancement of activities elicited by Spm in respect to BD23. These data suggest that, although BD23 and Spm show an over-all similar biological profile the additional pyridine group of BD23, slightly affects the physiological characteristics. Taken together, our data suggest a strict relationship between Spm and its deriva-tive BD23 and ROS concentration, in which also the Ca^{2+}-gradient is involved. ROS are known to play key roles in modulating cell wall extensibility, that must be loosen enough to allow expansion but also strong enough to prevent tip bursting [56]. Our results show that decreased ROS level promotes loss of polarity and induces tip swelling, probably altering the balance between ROS that promotes wall stiffening and relaxation [25]. This suggests that $O_2^{\bullet-}$ and H_2O_2 may play a role in modulating cell wall strengthening.

Wu et al. [57] reported that Spd might enter pollen tubes and induce an accumulation of H_2O_2 as result of oxidation mechanisms involving the activity of enzymes such as PAO. The increase of H_2O_2 might in turn stimulate the opening of hyperpolarization-activated Ca^{2+} channels in the plasma membrane leading to an increase of cytosolic Ca^{2+}. Accumulation of Ca^{2+} may trigger a series of dra-matic effects on the actin cytoskeleton such as depolymerisation. In the present work, Spm might cause comparable effects. Spm can be potentially subjected to oxidation processes thereby leading to accumulation of H_2O_2. Catabolism of Spm may also lead to produc-tion of Spd, which can in turn increase the content of H_2O_2 [57]. Therefore, the effects of Spm on cytosolic Ca^{2+} might be mediated by the levels of ROS, at least until the concentration of ROS is re-equilibrated by the ROS-scavenging system based on SOD and CAT. If an excess of Ca^{2+} enter the pollen tube, the mechanism supporting Ca^{2+} gradient is unbalanced with fast (about 1 min after the SI) and dramatic consequence on pollen tube growth as shown in *Papaver rhoeas* pollen tubes after self-incompatibility (SI) response [58].

Therefore, Spm and BD23 could alter the pollen tube tip morphology either directly by being covalently linked to wall com-
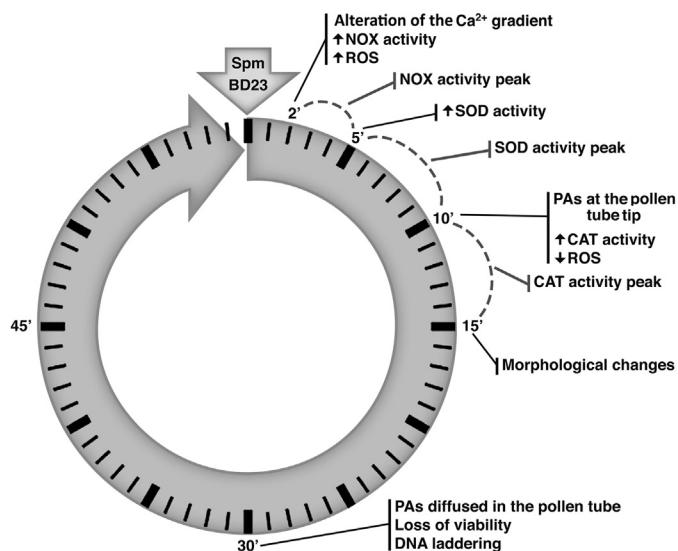

Fig. 12. From exogenous PAs supply to cell death: an overview of the timing. After 10 min from Spm and BD23 supply, the Ca^{2+} apical gradient was altered and NOX activity increased, with a maximum peak within 2 and 5 min. At 5 min SOD activ-ity was increased with a maximum peak within 5 and 10 min, depending on the PAs supplied. At 10 min PAs localized at the tip of the pollen tube then they diffuse along the subapical region. At 10 min, CAT activity was stimulated and ROS concen-tration decreased. At 15 min, signs of morphological changes start to be visible and at 30 min, DNA laddering occurred followed by cell death.

ponents through TGase or indirectly by altering ROS concentration and perturbing Ca^{2+} influx. The final event of Spm supplementation was DNA laddering and the degradation of the nuclei (especially the vegetative one usually located at the tip region) thus leading to cell death. This could be induced by the altered redox state or by Ca^{2+}-activated signaling; however, the possibility that PAs affect nuclear DNA stability, as suggested by well-established literature data, cannot be ruled out [9,10]. Moreover, the shorter distance between DAPI-stained nuclei of treated pollen might depend on the male germ unit not efficiently transported by the cytoskele-ton, as it occurs in untreated samples. In the attempt to provide a timeline of events occurring after supplementation of Spm, we have depicted a hypothetical sequence in Fig. 12.

Altogether, these results show how fine-tuned must be the mod-ulation of free and conjugated PAs, and show that the level of PAs is regulated by different processes such as catabolism, biosynthesis, conjugation, inter-conversion and transport. The PA homeostasis is essential for a proper pollen tube growth because it controls ROS titre, whose balance is controlled by production and scavenging. Furthermore, these findings may contribute to give a new spark in understanding the intricate networks involved in pollen tube ger-mination, and how the major players involved in this process (PAs, ROS, cytoskeleton and Ca^{2+}) could be interconnected.

References

[1] A.F. Tiburcio, T. Altabella, M. Bitrian, R. Alcazar, The roles of polyamines during the lifespan of plants: from development to stress, Planta 240 (2014) 1–18.
[2] A. Takano, J. Kakehi, T. Takahashi, Thermospermine is not a minor polyamine in the plant kingdom, Plant Cell Physiol. 53 (2012) 606–616.

[3] S. Del Duca, D. Serafini-Fracassini, G. Cai, Senescence and programmed cell death in plants: polyamine action mediated by transglutaminase, Front. Plant Sci. 5 (2014) 120.

[4] R. Walden, A. Cordeiro, A.F. Tiburcio, Polyamines: small molecules triggering pathways in plant growth and development, Plant Physiol. 113 (1997) 1009–1013.

[5] P.N. Moschou, K.A. Roubelakis-Angelakis, Polyamines and programmed cell death, J. Exp. Bot. 65 (2014) 1285–1296.

[6] G. Cai, E. Sobieszczuk-Nowicka, I. Aloisi, L. Fattorini, D. Serafini-Fracassini, et al., Polyamines are common players in different facets of plant programmed cell death, Amino Acids 47 (2015) 27–44.

[7] N.T. Dutra, V. Silveira, I.G. de Azevedo, L.R. Gomes-Neto, A.R. Facanha, et al., Polyamines affect the cellular growth and structure of pro-embryogenic masses in *Araucaria angustifolia* embryogenic cultures through the modulation of proton pump activities and endogenous levels of polyamines, Physiol. Plant 148 (2013) 121–132.

[8] B. Belda-Palazon, L. Ruiz, E. Marti, S. Tarraga, A.F. Tiburcio, et al., Aminopropyltransferases involved in polyamine biosynthesis localize preferentially in the nucleus of plant cells, PLoS One 7 (2012) e46907.

[9] H.C. Ha, N.S. Sirisoma, P. Kuppusamy, J.L. Zweier, P.M. Woster, et al., The natural polyamine spermine functions directly as a free radical scavenger, Proc. Natl. Acad. Sci. U. S. A. 95 (1998) 11140–11145.

[10] K.C. Das, H.P. Misra, Hydroxyl radical scavenging and singlet oxygen quenching properties of polyamines, Mol. Cell. Biochem. 262 (2004) 127–133.

[11] R. Minocha, R. Majumdar, S.C. Minocha, Polyamines and abiotic stress in plants: a complex relationship, Front. Plant Sci. 5 (2014) 175.

[12] E.A. Andronis, P.N. Moschou, I. Toumi, K.A. Roubelakis-Angelakis, Peroxisomal polyamine oxidase and NADPH-oxidase cross-talk for ROS homeostasis which affects respiration rate in *Arabidopsis thaliana*, Front. Plant Sci. 5 (2014) 132.

[13] G. Cai, M. Cresti, Organelle motility in the pollen tube: a tale of 20 years, J. Exp. Bot. 60 (2009) 495–508.

[14] S. Del Duca, D. Serafini-Fracassini, P. Bonner, M. Cresti, G. Cai, Effects of post-translational modifications catalysed by pollen transglutaminase on the functional properties of microtubules and actin filaments, Biochem. J. 418 (2009) 651–664.

[15] M.M. Wudick, J.A. Feijo, At the intersection: merging Ca^{2+} and ROS signaling pathways in pollen, Mol. Plant 7 (2014) 1595–1597.

[16] N. Bagni, P. Adamo, D. Serafini-Fracassini, RNA, proteins and polyamines during tube growth in germinating apple pollen, Plant Physiol. 68 (1981) 727–730.

[17] A. Speranza, G.L. Calzoni, Compounds released from incompatible apple pollen during in vitro germination, Z. Pflanzenphysiol. 97 (1980) 95–102.

[18] F. Antognoni, N. Bagni, Bis(guanylhydrazones) negatively affect in vitro germination of kiwifruit pollen and alter the endogenous polyamine pool, Plant Biol. (Stuttg.) 10 (2008) 334–341.

[19] A. Di Sandro, S. Del Duca, E. Verderio, A.J. Hargreaves, A. Scarpellini, et al., An extracellular transglutaminase is required for apple pollen tube growth, Biochem. J. 429 (2010) 261–271.

[20] A. Speranza, R. Crinelli, V. Scoccianti, A. Geitmann, Reactive oxygen species are involved in pollen tube initiation in kiwifruit, Plant Biol. (Stuttg.) 14 (2012) 64–76.

[21] S. Swanson, S. Gilroy, ROS in plant development, Physiol. Plant 138 (2010) 384–392.

[22] I. Pottosin, A.M. Velarde-Buendia, I. Zepeda-Jazo, O. Dobrovinskaya, S. Shabala, Synergism between polyamines and ROS in the induction of $Ca^{(2+)}$ and $K^{(+)}$ fluxes in roots, Plant Signal. Behav. 7 (2012) 1084–1087.

[23] M. Potocky, M.A. Jones, R. Bezvoda, N. Smirnoff, V. Zarsky, Reactive oxygen species produced by NADPH oxidase are involved in pollen tube growth, New Phytol. 174 (2007) 742–751.

[24] J. Foreman, V. Demidchik, J.H. Bothwell, P. Mylona, H. Miedema, et al., Reactive oxygen species produced by NADPH oxidase regulate plant cell growth, Nature 422 (2003) 442–446.

[25] I. Pottosin, S. Shabala, Polyamines control of cation transport across plant membranes: implications for ion homeostasis and abiotic stress signaling, Front. Plant Sci. 5 (2014) 154.

[26] C. Melchiorre, A. Cassinelli, W. Quaglia, Differential blockade of muscarinic receptor subtypes by polymethylene tetraamines. Novel class of selective antagonists of cardiac M-2 muscarinic receptors, J. Med. Chem. 30 (1987) 201–204.

[27] A. Minarini, A. Milelli, V. Tumiatti, M. Rosini, M.L. Bolognesi, et al., Synthetic polyamines: an overview of their multiple biological activities, Amino Acids 38 (2010) 383–392.

[28] R. Saiki, Y. Yoshizawa, A. Minarini, A. Milelli, C. Marchetti, et al., In vitro and in vivo evaluation of polymethylene tetraamine derivatives as NMDA receptor channel blockers, Bioorg. Med. Chem. Lett. 23 (2013) 3901–3904.

[29] B.G. Forde, M.R. Roberts, Glutamate receptor-like channels in plants: a role as amino acid sensors in plant defence? F1000Prime Rep. 6 (2014) 37.

[30] E. Bonaiuto, A. Minarini, V. Tumiatti, A. Milelli, M. Lunelli, et al., Synthetic polyamines as potential amine oxidase inhibitors: a preliminary study, Amino Acids 42 (2012) 913–928.

[31] E. Bonaiuto, A. Milelli, G. Cozza, V. Tumiatti, C. Marchetti, et al., Novel polyamine analogues: from substrates towards potential inhibitors of monoamine oxidases, Eur. J. Med. Chem. 70 (2013) 88–101.

[32] A. Minarini, A. Milelli, V. Tumiatti, M. Rosini, M. Lenzi, et al., Exploiting RNA as a new biomolecular target for synthetic polyamines, Gene 524 (2013) 232–240.

[33] A. Minarini, R. Budriesi, A. Chiarini, C. Melchiorre, V. Tumiatti, Further investigation on methoctramine-related tetraamines: effects of terminal N-substitution and of chain length separating the four nitrogens on M2 muscarinic receptor blocking activity, Farmaco 46 (1991) 1167–1178.

[34] S. Del Duca, A.M. Bregoli, C. Bergaini, D. Serafini-Fracassini, Transglutaminase-catalyzed modification of cytoskeletal proteins by polyamines during the germination of *Malus domestica* pollen, Sexual Plant Reprod. 10 (1997) 89–95.

[35] C.J. Weydert, J.J. Cullen, Measurement of superoxide dismutase, catalase and glutathione peroxidase in cultured cells and tissue, Nat. Protoc. 5 (2010) 51–66.

[36] M. Sagi, R. Fluhr, Superoxide production by plant homologues of the gp91(phox) NADPH oxidase. Modulation of activity by calcium and by tobacco mosaic virus infection, Plant Physiol. 126 (2001) 1281–1290.

[37] S. Pasqualini, E. Tedeschini, G. Frenguelli, N. Wopfner, F. Ferreira, et al., Ozone affects pollen viability and NAD(P)H oxidase release from *Ambrosia artemisiifolia* pollen, Environ. Pollut. 159 (2011) 2823–2830.

[38] A. Daudi, Z. Cheng, J.A. O'Brien, N. Mammarella, S. Khan, et al., The apoplastic oxidative burst peroxidase in Arabidopsis is a major component of pattern-triggered immunity, Plant Cell 24 (2012) 275–287.

[39] X.L. Wang, T. Takai, S. Kamijo, H. Gunawan, H. Ogawa, et al., NADPH oxidase activity in allergenic pollen grains of different plant species, Biochem. Biophys. Res. Commun. 387 (2009) 430–434.

[40] B.D. Lade, A.S. Patil, H.M. Paikrao, Efficient genomic DNA extraction protocol from medicinal rich *Passiflora foetida* containing high level of polysaccharide and polyphenol, Springerplus 3 (2014) 457.

[41] I. Pottosin, A.M. Velarde-Buendia, J. Bose, I. Zepeda-Jazo, S. Shabala, et al., Cross-talk between reactive oxygen species and polyamines in regulation of ion transport across the plasma membrane: implications for plant adaptive responses, J. Exp. Bot. 65 (2014) 1271–1283.

[42] R.A. Iorio, A. Di Sandro, R. Paris, G. Pagliarani, S. Tartarini, et al., Simulated environmental criticalities affect transglutaminase of Malus and Corylus pollens having different allergenic potential, Amino Acids 42 (2012) 1007–1024.

[43] P.C. Tomar, N. Lakra, S.N. Mishra, Cadaverine: a lysine catabolite involved in plant growth and development, Plant Signal. Behav. 8 (2013), http://dx.doi.org/10.4161/psb.25850

[44] K. Sorkheh, B. Shiran, V. Rouhi, M. Khodambashi, J.N. Wolukau, et al., Response of in vitro pollen germination and pollen tube growth of almond (*Prunus dulcis* Mill.) to temperature, polyamines and polyamine synthesis inhibitor, Biochem. Syst. Ecol. 39 (2011) 749–757.

[45] R. Biasi, G. Falasca, A. Speranza, A. De Stradis, V. Scoccianti, et al., Biochemical and ultrastructural features related to male sterilityin the dioecious species *Actinidia deliciosa*, Plant Physiol. Biochem. 39 (2001) 395–406.

[46] P. Mariani, D. D'Orazi, N. Bagni, Polyamines in primary wall of carrot cells: endogenous content and interactions, J. Plant Physiol. 135 (1989) 508–510.

[47] E. Grienenberger, S. Besseau, P. Geoffroy, D. Debayle, D. Heintz, et al., A BAHD acyltransferase is expressed in the tapetum of Arabidopsis anthers and is involved in the synthesis of hydroxycinnamoyl spermidines, Plant J. 58 (2009) 246–259.

[48] D. Serafini-Fracassini, S. Del Duca, Transglutaminases: widespread cross-linking enzymes in plants, Ann. Bot. 102 (2008) 145–152.

[49] S. Del Duca, C. Faleri, R.A. Iorio, M. Cresti, D. Serafini-Fracassini, et al., Distribution of transglutaminase in pear pollen tubes in relation to cytoskeleton and membrane dynamics, Plant Physiol. 161 (2013) 1706–1721.

[50] I. Zepeda-Jazo, A.M. Velarde-Buendia, R. Enriquez-Figueroa, J. Bose, S. Shabala, et al., Polyamines interact with hydroxyl radicals in activating $Ca^{(2+)}$ and $K^{(+)}$ transport across the root epidermal plasma membranes, Plant Physiol. 157 (2011) 2167–2180.

[51] L.F. Olsen, O.G. Issinger, B. Guerra, The Yin and Yang of redox regulation, Redox Rep. 18 (2013) 245–252.

[52] P. Schopfer, Hydroxyl radical-induced cell-wall loosening in vitro and in vivo: implications for the control of elongation growth, Plant J. 28 (2001) 679–688.

[53] J. Kubis, Polyamines and scavenging system: influence of exogenous spermidine on catalase and guaiacol peroxidase activities, and free polyamine level in barley leaves under water deficit, Acta Physiol. Plant 25 (2003) 337–343.

[54] J. Kubis, The effect of exogenous spermidine on superoxide dismutase activity, H_2O_2 and superoxide radical level in barley leaves under water deficit conditions, Acta Physiol. Plant 27 (2005) 289–295.

[55] M. Fujita, K. Shinozaki, Identification of polyamine transporters in plants: paraquat transport provides crucial clues, Plant Cell Physiol. 55 (2014) 855–861.

[56] K. Muller, A. Linkies, R.A. Vreeburg, S.C. Fry, A. Krieger-Liszkay, et al., In vivo cell wall loosening by hydroxyl radicals during cress seed germination and elongation growth, Plant Physiol. 150 (2009) 1855–1865.

[57] J. Wu, Z. Shang, X. Jiang, P.N. Moschou, W. Sun, et al., Spermidine oxidase-derived H_2O_2 regulates pollen plasma membrane hyperpolarization-activated Ca^{2+} -permeable channels and pollen tube growth, Plant J. 63 (2010) 1042–1053.

[58] J. Wu, S. Wang, Y. Gu, S. Zhang, S.J. Publicover, et al., Self-incompatibility in Papaver rhoeas activates nonspecific cation conductance permeable to Ca^{2+} and K^+, Plant Physiol. 155 (2011) 963–973.